

BUOYANCY EFFECTS ON OPPOSING LAMINAR FLOW IN A UNIFORMLY HEATED INCLINED CYLINDER

Dr. Abdul hassan A. Karamallah
Prof.

University of Technology
Mechanical Eng. Dep.

Dr. Akeel A. Mohammed

University of Technology
Mechanical Eng. Dep.

Ameer A. Jadooa
Teaching Assistant.

University of Technology
Electromechanical Eng. Dep

ABSTRACT:

Experiments have been performed to investigate mixed convection heat transfer in the thermal and hydrodynamic entrance region of a uniformly heated inclined tube. The effects of surface heat flux, Reynolds number, the direction of main flow relative to secondary flow (opposing flow), and angle of tube inclination on the temperature distribution and local Nusselt number along tube were studied. The study covered Reynolds number range ($450 \leq Re \leq 2008$), and heat flux range ($95 \leq q \leq 898$) W/m^2 , Raylight number from 1.1132×10^5 to 3.6982×10^5 and angle of inclination $\alpha=0^\circ$ (Horizontal), $\alpha=30^\circ$, $\alpha=60^\circ$ (Inclined), $\alpha=90^\circ$ (Vertical). Results show that the heat transfer process improve whenever move angle of inclination from vertical position to horizontal position . The experimental data were correlated for Nu_m as a function of Ra_m & Re_m for each angle of inclination and then superimposed the angle of inclination α to give a general equation of average Nusselt number at any α in opposing flow.

Key words: Mixed Convection, Opposing Flow, cylinder, inclined .

الخلاصة:

اجريت تجارب عملية لدراسة عملية انتقال الحرارة بالحمل المختلط بمنطقة الدخول الهيدروديناميكية والحرارية لأنبوب مائل مسخن تسخين منتظم. تم دراسة تأثير الفيض الحراري للسطح ورقم رينولدز واتجاه الجريان الرئيسي نسبة الى الجريان الثانوي (جريان معاكس) على كل من تغير درجة حرارة سطح الأنبوب ورقم نسلت الموقعي على طول الأنبوب. غطت الدراسة رقم رينولدز ($450 \leq Re \leq 2008$) و فيض حراري ($95 \leq q \leq 898$) W/m^2 ورقم رايلي 1.1132×10^5 to 3.6982×10^5 وزوايا ميلان (عمودي $\alpha=90^\circ$ ، 60° ، 30° ، أفقي $\alpha=0^\circ$) بينت النتائج ان عملية انتقال الحرارة تتحسن مع الميل من الوضع العمودي الى الوضع الأفقي. تم استنباط معادلة تجريبية من البيانات العملية لمعدل رقم نسلت كدالة لرقم رينولدز Re ورقم Ra ، وزوايا الميلان α

INTRODUCTION:

Laminar flow heat transfer in tubes is encountered in a wide variety of engineering situations, including heat exchangers designed for various liquids in chemical process and food industries, compact heat exchanger for gas flow, and heat exchangers for biomedical applications. Even though such heat exchangers are now being used widely, there is a lack of understanding of many details of laminar flow and heat transfer. Many authors (such as Eckert and Diaguila 1953; Jackson, Harrison and Boteler 1958; Zeldin and Schmidt 1972; Hiroaki 1987) studied this problem to give an actual insite to the physic behavior of flow heat transfer. Mc Comas and Eckert [1966] studied experimentally the fully developed air flow in a uniformly heated tube for the Reynolds Number rang of approximately 900 down to 100.

The Grashof number was varied from 1000 down to the order one. Variation of the wall and bulk air temperatures and the local Nusselt numbers along the axial location x/d were depicted. For all the lower Reynolds number values, the experimental data show a shorter thermal entrance length than predicted. Cheng And Yuen [1982], submitted photographs for secondary flow patterns in the thermal entrance region of isothermally heated inclined tube wall temperature $T_w=55-95^\circ\text{C}$, air entrance temperature $t_i =25^\circ\text{C}$ for inverse Graetz number $Z=0.088-1.833$ $Re=3134-14$ and inclination angles from horizontal direction $\alpha=30^\circ, 45^\circ, 60^\circ$ at three wall temperature levels with upward laminar flow. The characteristic features of the secondary flow induced by buoyancy forces for Graetz problem in inclined tubes with significant free convection effects including its decay process and subsequent banishment in the downstream region were clearly delineated by the flow visualization studies. Akeel [1999], performed experiments to study the local heat transfer by mixed convection to a simultaneously developing air flow in a vertical and horizontal cylinder for $L/D=30$ and Reynolds number ranged from (420 to 1540) and heat flux varied from 62 W/m^2 to 370 W/m^2 . The results demonstrate an increase in the Nusselt number values along the cylinder as the heat flux increases and as the cylinder moves from vertical to the horizontal position. He performed also theoretical investigation of an axially symmetric, laminar air flow in an entrance region of a vertical cylinder, by solving in two directions the continuity, momentum and energy equations using implicit finite difference method and Gauss elimination technique. A comparison was made between the experimental and theoretical results for local Nusselt variation with the inverse Graetz number and gave the same trend and behavior. Mohammed and Yusaf [2006], performed an experiment as an extension line to the work of Akeel [1999], to investigate the effect of the flow pattern on the mixed convection heat transfer. A forced convection at the entrance region of a fully developed opposing laminar air flow was studied in this paper investigated to evaluate the flow direction effect on the Nusselt number. The Reynolds number ranged from 410 to 1600 and heat flux varied from 63 W/m^2 to 1260 W/m^2 , with different angles of tube inclination of $30^\circ, 45^\circ, 60^\circ$, and 90° . It was found that the surface temperature variation along the tube for opposed flow higher than the assisted flow but lower than the horizontal orientation. The Reynolds number has a significant effect on Nusselt number in opposed flow while the effect of Reynolds number was found to be small in the case of assisted flow. The Nusselt number values were lower for opposed flow than the assisted flow. The temperature profiles results have revealed that the secondary flows created by natural convection have a significant effect on the heat transfer process. The heat transfer data were correlated.

EXPERIMENTAL APPARATUS:

An experimental rig was designed and constructed to study the heat transfer process by mixed convection to a simultaneously hydrodynamic and thermal developing air flow in an inclined cylinder. The purpose of constructing this rig was to deduce an empirical equation of average Nusselt number in an opposing flow case as a function of Reynolds number, Rayleigh number, and angle of cylinder inclination. The experimental apparatus as shown in Fig.(1) consists essentially of cylinder as a test section as apart of an open air loop, mounted on an iron frame (I) which can be rotated around a horizontal spindle. The inclination angle of the cylinder can thus be adjusted

as required. An open air circuit was used which included a centrifugal fan (B), orifice plate section (C), settling chamber (F), test section and a flexible hose (E). The air which is driven by a centrifugal fan can be regulated accurately by using a control valve and enters the orifice pipe section (British Standard Unit) and then settling chamber through a flexible hose (E). The settling chamber was carefully designed to reduce the flow fluctuation and to get a uniform flow at the test section entrance by using flow straightener (G). The air then passed through 1.2 m long test section.

A symmetric flow and a uniform velocity profile produced by a well designed Teflon bell mouth (H) which is fitted at the beginning of aluminum cylinder (N) and bolted in the other side inside the settling chamber (F). Another Teflon piece (H) represents the cylinder exit and has the same dimensions as the inlet piece. The Teflon was chosen because its low thermal conductivity in order to reduce the heat losses from the aluminum cylinder ends. The inlet air temperature was measured by one thermocouple located in the settling chamber (F) while the outlet bulk air temperature was measured by two thermocouples located in the test section exit (R). The local bulk air temperature was calculated by using a straight line interpolation between the measured inlet and outlet bulk air temperature. The test section consists of 7.5 mm wall thickness, 59.3 mm outside diameter and 1.2m long aluminum cylinder. The cylinder was heated electrically using an electrical heater whose consists of 1 mm in diameter and 60 m in length nickel-chrome wire (L) electrically isolated by ceramic beads, wounds uniformly as a coil with 10 mm pitch. The outside of the test section was then thermally insulated, covered with 60 mm and 5.7 mm as thickness for asbestos rope layer and fiber glass, respectively. To enable the calculation of heat loss through the lagging to be carried out, six thermocouples are inserted in the lagging as two thermocouples at three points along the heated section 39 cm apart. Using the average measured temperature drop and thermal conductivity of lagging the heat losses through lagging can be calculated. The cylinder surface temperatures were measured by eighteen asbestos sheath thermocouple (type K). All the thermocouple wires and heater terminals were taken out the test section. To determine the heat loss from the test section ends, two thermocouples were fixed in each Teflon piece. Knowing the distance between these thermocouples and the thermal conductivity of the Teflon, the heat ends loss could thus be calculated. The thermocouple circuit consists of a digital electronic thermometer (type TM-200, serial no. 13528), connected in parallel to the thermocouples by leads through a selector switches. An orifice plate British Standard Unit (BSU) of diameter of (50 mm) and discharge coefficient of (0.6099) was used to compute the flow rate through the cylinder, by using the following equation.

$$\dot{V} = C_d \cdot (\pi D_o^2 / 4) \cdot \sqrt{2g\Delta h}$$

Where:

$$\dot{V} = \text{flow rate} = \text{mm}^3/\text{sec}$$

$$C_d = \text{discharge coefficient} = 0.6099$$

$$D_o = \text{diameter of orifice} = 50 \text{ mm}$$

EXPERIMENTAL PROCEDURE:

To carry out an experiment the following procedure was followed:

1. The inclination angle of the cylinder was adjusted as required.

2. The centrifugal fan was then switched on to circulate the air, through the open loop. A regulating valve was used for adjusting the required mass flow rate.
3. The electrical heater was switched on and the heater input power then adjusted to give the required heat flux.
4. The apparatus was left at least three hours to establish steady state condition. The thermocouples readings were measured every half an hour by means of the digital electronic thermometer until the reading became constant, a final reading was recorded. The input power to the heater could be increased to cover another run in a shorter period of time and to obtain steady state conditions for next heat flux and same Reynolds number. Subsequent runs for other Reynolds number and cylinder inclination angle ranges were performed in the same previous procedure.
5. During each test run , the following readings were recorded:
 - a. The angle of inclination of the cylinder in degree.
 - b. The reading of the manometer (air flow rate) in mm H₂O.
 - c. The readings of the thermocouples in °C.
 - d. The heater current in amperes.
 - e. The heater voltage in volts.

Data Analysis:

Simplified steps were used to analyze the heat transfer process for the air flow in a cylinder when its surface was subjected to a uniform heat flux.

The total input power supplied to the cylinder can be calculated:

$$Q_t = V \times I \tag{1}$$

The convection and radiation heat transferred from the cylinder is:

$$Q_{cr} = Q_t - Q_{cond} \tag{2}$$

Where Q_{cond} is the conduction heat loss which was found from the following equation:

$$Q_{cond} = \frac{\Delta T_{oi}}{\ln \frac{r_o}{r_i}} \cdot \frac{2 \pi k_a L}{1} \tag{3}$$

Where:

$$\Delta T_{oi} = T_o - T_i$$

T_o = average outer lagging surface temperature

T_i = average inner lagging surface temperature

r_o = the distance from center of cylinder to the outer lagging surface

r_i = the distance from center of cylinder to the beginning lagging (radius of outer cylinder surface)

L = length of cylinder

K_a = thermal conductivity of asbestos

The convection and radiation heat flux can be represented by:

$$q_{cr} = Q_{cr} / A_1 \tag{4}$$

Where:

$$A_1 = 2 \pi r_i L$$

The local radiation heat flux can be calculated as follows:

$$q_r = F_{1-2} \varepsilon \sigma \left[\left((T_s)_z + 273 \right)^4 - \left(\overline{(T_s)}_z + 273 \right)^4 \right] \quad (5)$$

Where:

$(T_s)_z$ = local temperature of cylinder.

$\overline{(T_s)}_z$ = average temperature of cylinder.

σ = steavan boltzman constant = $5.66 \times 10^{-8} \text{ W/m}^2 \text{ K}^4$

ε = emissivity of the polished aluminum surface = 0.09.

$F_{1-2} \approx 1$

Hence the convection heat flux at any position is:

$$q = q_{cr} - q_r \quad (6)$$

The radiation heat flux is very small equal 2% and can be neglected.

Hence:

$q_{cr} \approx q$ = convection heat flux

The local heat transfer coefficient can be obtained as:

$$h_z = \frac{q}{(T_s)_z - (T_b)_z} \quad (7)$$

$(T_b)_z$ = Local bulk air temperature.

$$(T_f)_z = \frac{(T_s)_z + (T_b)_z}{2} \quad (8)$$

$(T_f)_z$ = Local mean film air temperature.

The local Nusselt number (Nu_z) then can be determined as:

$$Nu_z = \frac{h_z D_h}{k} \quad (9)$$

Where:

k = thermal conductivity of air

The average values of Nusselt number Nu_m can be calculated as follows:

$$Nu_m = \frac{1}{L} \int_0^L Nu_z dz \quad (10)$$

The average values of the other parameters can be calculated based on calculation of average cylinder surface temperature and average bulk air temperature as follows:

$$\overline{(T_s)} = \frac{1}{L} \int_{z=0}^{z=L} (T_s)_z dz \quad (11)$$

$$\bar{T}_b = \frac{1}{L} \int_{z=0}^{z=L} (T_b)_z dz \quad (12)$$

$$\bar{T}_f = \frac{\bar{T}_s + \bar{T}_b}{2} \quad (14)$$

All the air physical properties ρ , μ , ν , and k were evaluated at the average mean film temperature (\bar{T}_f).

RESULTS AND DISCUSSION:

Temperature Variation:

Horizontal Position:

Generally, the variation of surface temperature along the surface cylinder may be affected by many variables such as heat flux, Reynolds number, and cylinder inclination angles.

The temperature variation in the horizontal position is plotted for selected runs in Figs.(2, 3, 4 and 5). Fig.(2) shows the variation of the surface temperature along cylinder for different heat flux and for $Re=450$. This figure reveals that the surface temperature increases at the cylinders entrance and attains a maximum point after which the surface temperature begins to decrease. The rate of surface temperature rises at early stage is directly proportional to the wall heat flux. This can be attributed to the increasing of the thermal boundary layer faster due to buoyancy effect as the heat flux increases for the same Reynolds number. The point of maximum temperature on the curve represents actually the starting of thermal boundary layer fully developed. The region before this point is called the entrance of cylinder, The same behavior seems in the Fig.(3) for Reynolds number 2008, but lower temperature because of dominant forced convection in the heat transfer process.

Figs.(4 & 5) show the effect of Reynolds number variation on the cylinder surface temperature for low heat flux ($q=145 \text{ W/m}^2$) in Fig.(4) and for high heat flux ($q=898 \text{ W/m}^2$) in Fig.(5); respectively. It is obvious that the increasing of Reynolds number reduces the surface temperature as heat flux kept constant. It is necessary to mention that as heat flux increases the cylinder surface temperature increases because the free convection is the dominating factor in the heat transfer process.

Vertical Position:

The variations of surface temperature along the axial distance for vertical cylinder ($\alpha=90^\circ$), ($Re=450$ & 2008), and for different heat flux are shown in Fig.(6) & Fig.(7); respectively, and for different Reynolds number with ($q=95 \text{ W/m}^2$ & $q=622 \text{ W/m}^2$), are show in Fig.(8) & Fig.(9) respectively; The effect of heat flux and Reynolds number on the cylinder temperature variation is the same as that obtained in the horizontal and inclined positions.

The extent of mixed convection depends on the magnitude of the heat flux and Reynolds number for the same angle of inclination. When heat flux and Reynolds number are kept constant, the extent of local mixing due to the buoyancy effect in horizontal cylinder is larger than other cylinder angles of inclination. It has been proved

that for the same condition of flow rate and input heat flux, the surface temperature variation along the cylinder decreases as the angle of inclination changes from vertical to horizontal position.

Angle of Inclination Effect on the Temperature Distribution:

The variations of cylinder surface temperature along the axial distance for the same Reynolds number and heat flux, and for different angles ($\alpha=0^\circ, 30^\circ, 60^\circ,$ and 90°) are shown in Figs.(10 to 13), respectively. Figures show a reduction in surface temperature with mean approximated value 13% as the angle of cylinder inclination moves from vertical to horizontal position; this can be attributed to the large buoyancy effect in a horizontal cylinder compared with the other cylinder angles of inclination. It is noticed from these figures that at the same axial distance the heat transfer process improve down stream as the angle of inclination moves from vertical to horizontal position.

Local Nusselt Number (Nu_x): Horizontal Position:

The variation of local Nusselt number (Nu_x) with a logarithmic dimensionless axial distance (inverse Graetz number, $ZZ = \frac{x/D_h}{Pr Re}$), for horizontal position is plotted, for a selected runs, in Figs.(14 to 16).

The effect of heat flux on the Nu_x for $Re=450$ is shown in Fig.(14). It is clear from this figure that at the higher heat flux, the results of the local Nusselt number are higher than the results of lower heat flux. This may be attributed to the secondary flow superimposed on the forced flow effect which increases as the heat flux increases leading to higher heat transfer coefficient.

The effects of Re on Nu_x variation with ZZ are shown in Figs.(15 & 16) for heat flux equal to 145 W/m^2 and 898 W/m^2 ; respectively. For constant heat flux, results depicted that the deviation of Nu_x value moves towards the left and increases as the Reynolds number increases because of decreasing of inverse Graetz number ZZ . This situation reveals the domination of forced convection on the heat transfer process which improves as Reynolds number increases.

Vertical Position:

The variations of the local Nusselt number with ZZ for different heat fluxes and Reynolds number equal to 450 and for different Reynolds numbers and heat fluxes equal to 95 & 622 W/m^2 are shown Figs.(17 to 19); respectively. Results reveal that the effect of heat flux and Reynolds number on heat transfer coefficient in vertical position gives a similar trend as obtained for horizontal and inclined position.

Angle of Inclination Effect on the Local Nusselt Number:

The effect of angle of inclination on the local Nusselt number variation for ($q=117 \text{ W/m}^2$ & $Re=450$) and ($q=705 \text{ W/m}^2$ & $Re=2008$) are shown in Fig.(20 & 21), respectively. This figure indicates that for all ZZ values, the Nu_x value for horizontal position is higher than that for opposing flow positions, with mean approximated value

9% between $\alpha=0^\circ$ and $\alpha=90^\circ$ in Fig.(20) and with mean approximated values 16% between $\alpha=0^\circ$ and $\alpha=90^\circ$ in Fig.(21). As explained before, where the buoyancy flow opposes forced flow, the local mixing will decrease and decreases as angle of inclination deviates from horizontal to vertical; leads to decreasing of heat transfer coefficient.

Average Nusselt Number :

Correlation of Average Heat Transfer Data;

The values of the average Nusselt number (Nu_m) for horizontal position ($\alpha=0^\circ$), inclined position for opposing flow ($\alpha= 30^\circ, 60^\circ$), and vertical position for opposing flow ($\alpha=90^\circ$) are plotted in Figs.(22 to 25) in the form of $\log(Nu_m)$ against $\log(Ra/Re)$ for the range of Re from 450 to 2008, and Ra from 1.1132×10^5 to 3.6982×10^5 . All the points as can be seen are represented by linearization of the following equations:

$\alpha=0^\circ$ (horizontal)	$Nu_m=2.962 (Ra/Re)^{-0.6369}$	(15)
$\alpha=30^\circ$	$Nu_m=2.131 (Ra/Re)^{-0.8055}$	(16)
$\alpha=60^\circ$	$Nu_m=2.891 (Ra/Re)^{-0.7224}$	(17)
$\alpha=90^\circ$ (vertical opposing flow)	$Nu_m=2.855 (Ra/Re)^{-0.7773}$	(18)

It was shown that the heat transfer equations for all the positions have the same following form:

$$Nu_m = a(Ra/Re)^d \quad (19)$$

Where a and d is shown in table (1):

Table (1): Constants In Eq.(19) For Various Angles of Inclination

α	a	d
0	2.962	-0.6369
30	2.131	-0.8055
60	2.891	-0.7224
90	2.855	-0.7773

Hence, a general correlation for the average Nusselt number as a function of parameters Ra , Re , and α is deduced as given below:

$$(Nu)_{inc.} = 7.4672 \cdot (Ra)^{-0.639} \cdot (Re)^{0.6432} \cdot (\alpha)^{-0.01265} \quad (20)$$

Where: α is measured in degree

CONCLUSIONS:

1. The variation of the surface temperature along the axial axis of cylinder at all angles of inclinations is affected by the extent of the local mixing which increases as the heat flux increases, Re decreases and cylinder orientation deviates from vertical to horizontal. The increase of local mixing causes an improvement in the local heat transfer process and reducing the heated surface temperature.

2. The variation of Nu_x with ZZ at any angle of inclination is affected by many variables summarized in the following points:
- a. For the same Re and cylinder orientation, the Nu_x increases with heat flux.
 - b. For the same heat flux and cylinder orientation the heat transfer process is dominated by:
 - i. Forced convection as Re increases and becomes relatively high if compared with the applied heat flux.
 - ii. Natural convection as Re decreases and becomes relatively low if compared with the applied heat flux.
 - c. For the same heat flux & Re , the Nu_x value decreases as cylinder position changes from horizontal towards vertical.
3. The effect of buoyancy is small at the cylinder entrance and increases in the flow direction.

REFERENCE

- [1] Akeel A. Mohamed "Combined free and forced convection in a circular cylinder", M.sc. thesis, university of Baghdad, college of engineering, mechanical department, (Oct.1999).
- [2] Cheng B. , Yuen D. Lasoos "Flow visualization studies on secondary flow pattern mixed convection in the thermal entrance region of isothermally heated inclined pipes" J.Heat Transfer, vo4.60 pp.121-129, (Des1982).
- [3] Eckert B. , Diaguila E. Lebart "Convective heat transfer for mixed, free, and forced flow thought tubes" J.Heat Transfer, vo2.30,pp.497-504, (Sep.1953).
- [4] Hiroaki R. Brateal, Et-Al "Combined forced and natural convection heat transfer for upward flow in a uniformly heated vertical pipe" J.Heat Mass Transfer, vol.30, No.1, pp.165-174, (Nov.1987).
- [4] Jackson T. Crevan, Harrison L. Spreven and Boteler "Combined free and forced convection in a constant-temperature vertical tube" ASME Tran.vol.80, pp.739-745,(Fab1958).
- [5] Mccomas F. leman , Eckert H. K. "Combined free and forced convection in a horizontal circular tube" J.Heat Transfer, vo2.99, pp.147-153, (Sep..1966).
- [6] Mohammed , Yusaf "Heat transfer by mixed convection opposing laminar flow from the inside surface of uniformly heated inclined circular tube" ASME,university of tenaga nasional,(Oct.2006)
- [7] Zeldin N. Monvera , Schmidt L. X. "Developing flow with combined forced-free convection in an isothermally vertical tube" J.Heat Transfer, (May 1972).

NOMENCLATURE:

Latin Symbols:

Symbol	Description	Unit
A_c	Cylinder cross section area	(m ²)
A_s	Cylinder surface area	(m ²)
C_p	Specific heat at constant pressure	(J/Kg.°C)
D_h	Hydraulic diameter	(m)
G	Gravitational acceleration	(m/s ²)
H	Coefficient of heat transfer	(W/m ² .°C)
I	Current	(amp)
K	Thermal conductivity	(W/m ² .°C)
K_a	Thermal conductivity of asbestos	(W/m ² .°C)
L	Cylinder length	(m)
\dot{V}	Volumetric flow rate	(m ³ /s)
Q	Convection heat flux	(W/m ²)
Q_{cond}	Conduction heat loss	(W)
Q_t	Total heat given	(W)
r_i	Inner radius of cylinder	(m)
r_o	The distance from center of cylinder to the outer lagging surface	(cm)
r_i	The distance from center of cylinder to the beginning lagging (radius of outer cylinder surface)	(cm)
t_b	Bulk air temperature	(°C)
t_f	Mean film air temperature	(°C)
t_i	Air temperature at cylinder entrance	(°C)
t_s	Cylinder surface temperature	(°C)
v	Voltage	(Volt)
x	Axial coordinate	(m)

Creek Symbols:

α	cylinder Inclined angle	(degree)
μ	Dynamic viscosity	(Kg/m.s)
ν	Kinematics viscosity	(m ² /s)
ρ	Air density at any point	(Kg/m ³)

Subscript:

°	Degree
x	Local
m	Average

Dimensionless Gropes:

Gr	Grashof number	$\frac{g\beta(t_s - t_b)D_h^3}{\nu^2}$
Nu	Nusselt number	$\frac{hD_h}{k}$

Pr,	Prandtal number	$\frac{\mu C_p}{k}$
Ra,	Rayligh number	Gr.Pr
Re,	Reynolds number	$\frac{u_i D_h}{\nu}$
G _z	Graetz number	Re.Pr.D _h / x
ZZ,	Axial distance	x/Re.Pr.D _h

A	Electrical Motor
B	Centrifugal Fan
C	Orifice
D	Manometer
E	Flexible Hose
F	Settling Chamber
G	Straightener
H	Beel Mouth
I	Iron Fral...
J	Asbestos
K	Thermocouple
L	Heater
M	Instrument Used
N-N	Cylinder

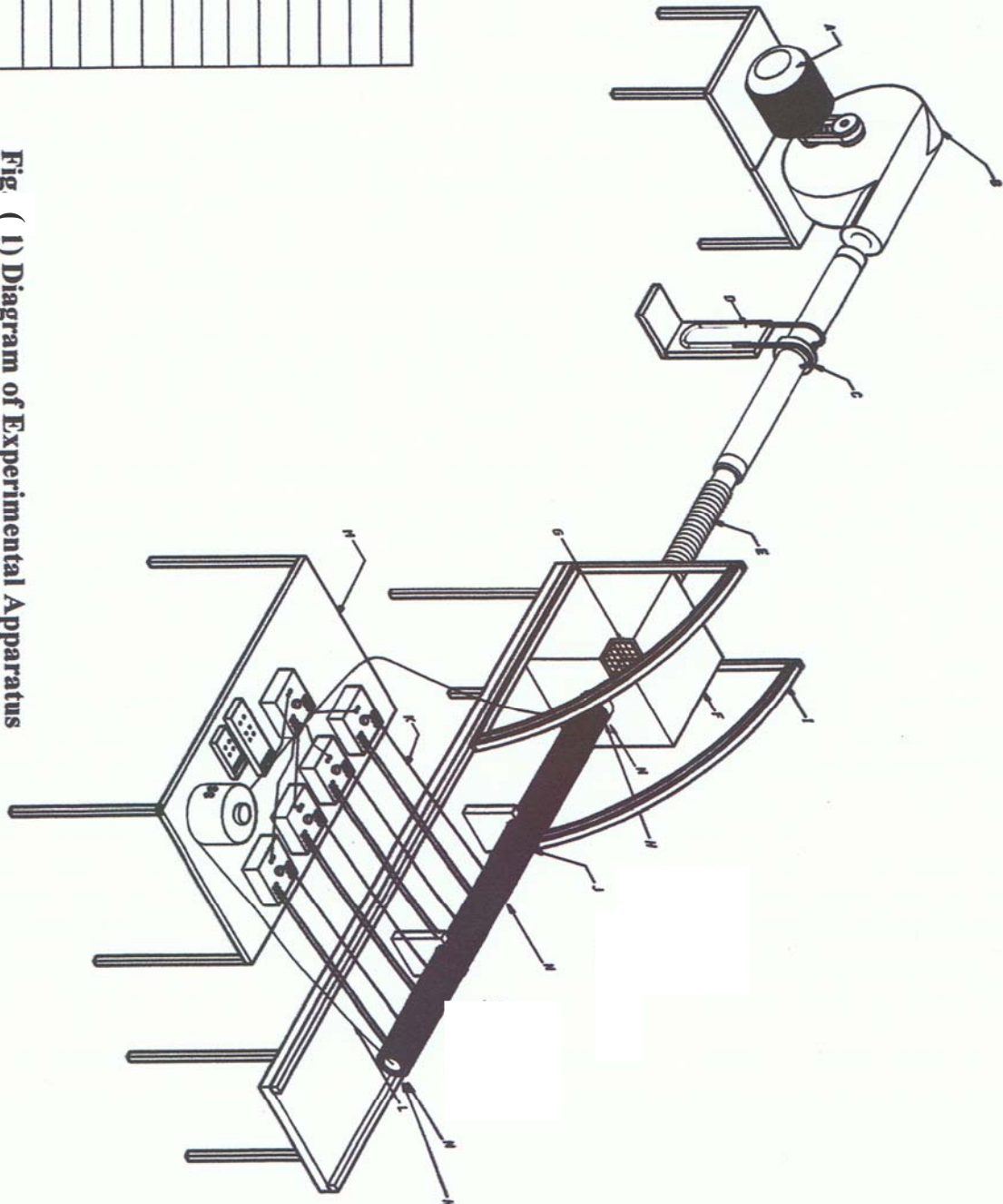


Fig (1) Diagram of Experimental Apparatus

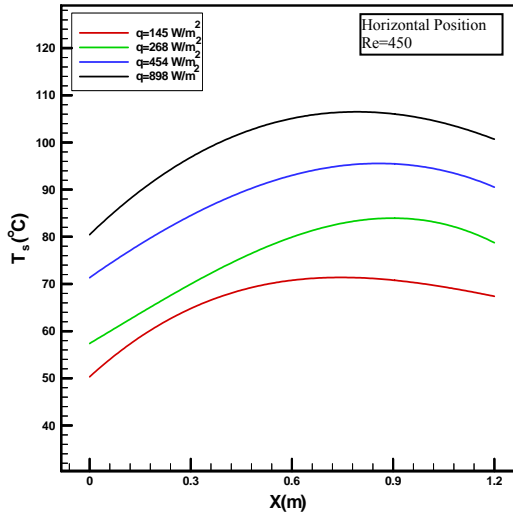


Fig.(2): Experimental Variation of the Surface Temperature with the Axial Distance, $Re=450$, $\alpha = 0^\circ$ (Horizontal).

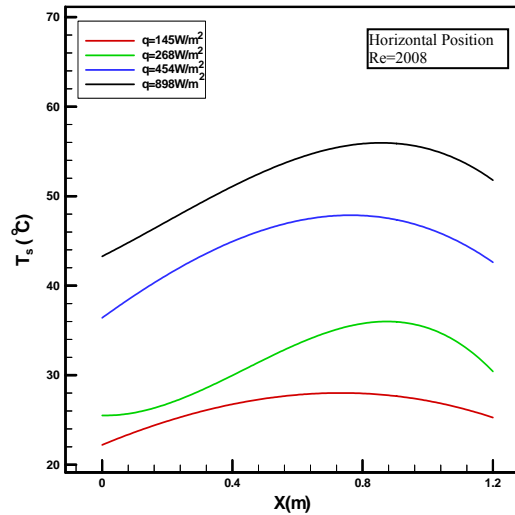


Fig.(3): Experimental Variation of the Surface Temperature with the Axial Distance, $Re=2008$, $\alpha = 0^\circ$ (Horizontal).

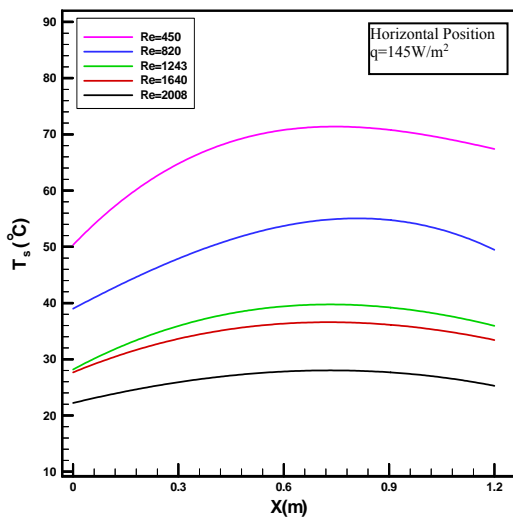


Fig.(4): Experimental Variation of the Surface Temperature with the Axial Distance, $q=145W/m^2$, $\alpha = 0^\circ$ (Horizontal).

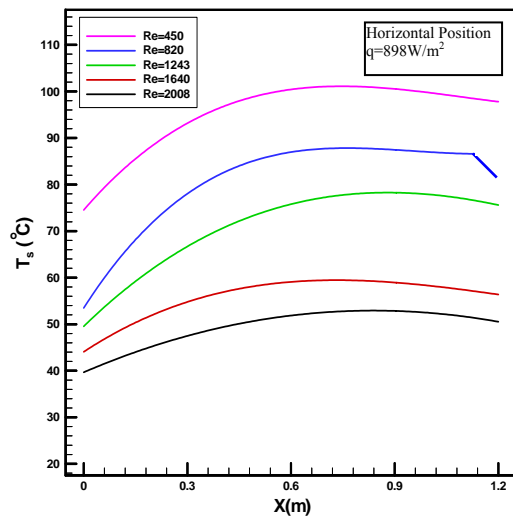


Fig.(5): Experimental Variation of the Surface Temperature with the Axial Distance, $q=898W/m^2$, $\alpha = 0^\circ$ (Horizontal).

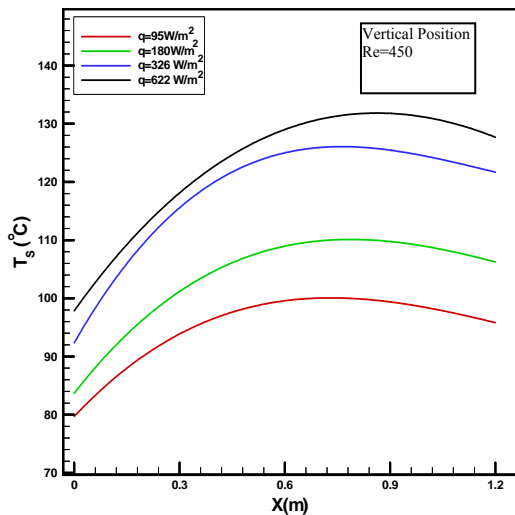


Fig. (6): Experimental Variation of the Surface Temperature with the Axial Distance, $Re=450$, $\alpha = 90^\circ$ (Vertical).

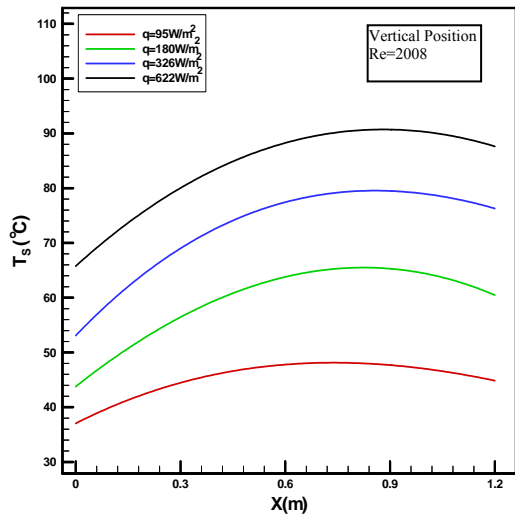


Fig.(7): Experimental Variation of the Surface Temperature with the Axial Distance, $Re=2008$, $\alpha = 90^\circ$ (Vertical).

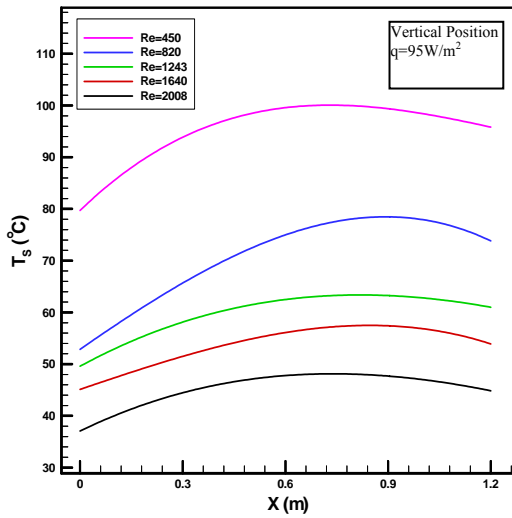


Fig.(8): Experimental Variation of the Surface Temperature with the Axial Distance, $q=95W/m^2$, $\alpha = 90^\circ$ (Vertical).

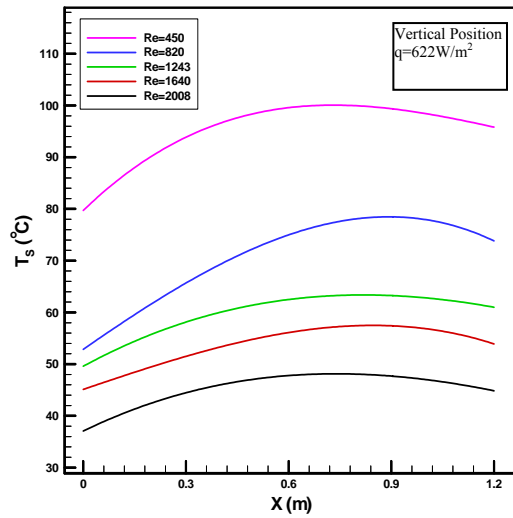


Fig.(9): Experimental Variation of the Surface Temperature with the Axial Distance, $q=622W/m^2$, $\alpha = 90^\circ$ (Vertical).

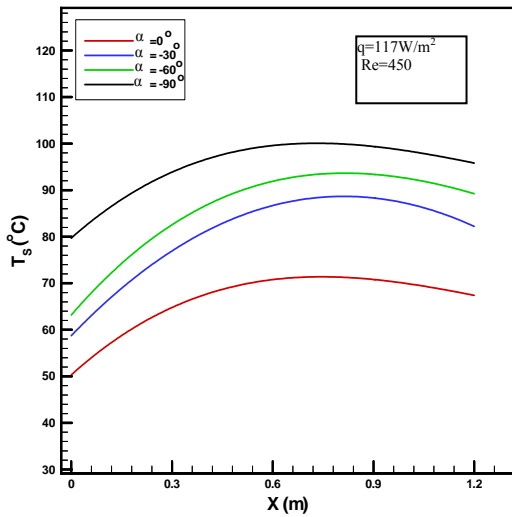


Fig.(10): Experimental Variation of the Surface Temperature with the Axial Distance for Various Angles, $q=117W/m^2$, $Re=450$.

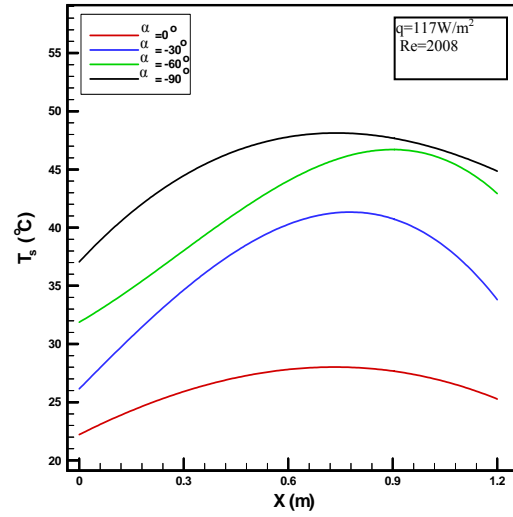


Fig.(11): Experimental Variation of the Surface Temperature with the Axial Distance for Various Angles, $q=117W/m^2$, $Re=2008$.

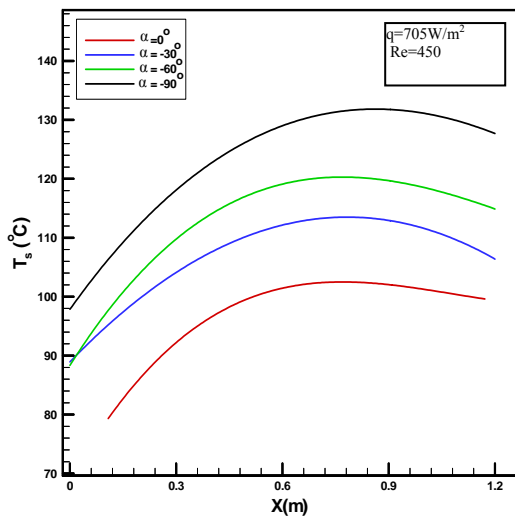


Fig.(12): Experimental Variation of the Surface Temperature with the Axial Distance for Various Angles, $q=705W/m^2$, $Re=450$.

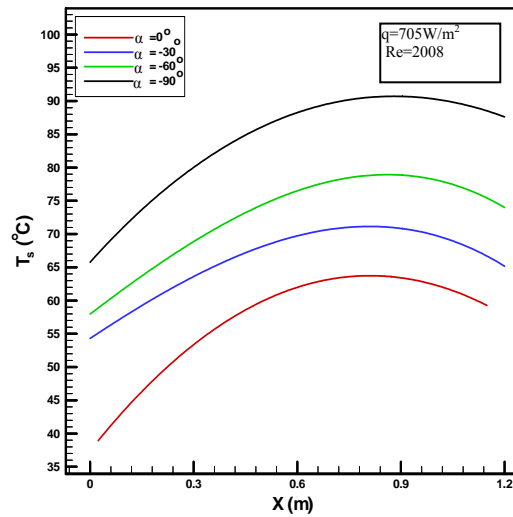


Fig.(13): Experimental Variation of the Surface Temperature with the Axial Distance for Various Angles, $q=705W/m^2$, $Re=2008$.

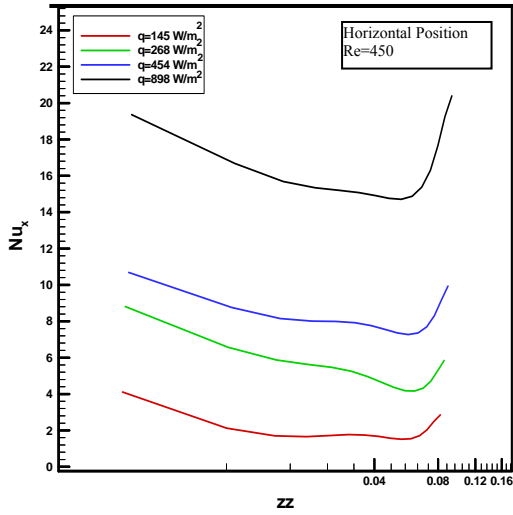


Fig.(14): Experimental Local Nusselt number Versus Dimensionless Axial Distance, $Re=450$, $\alpha = 0^\circ$ (Horizontal).

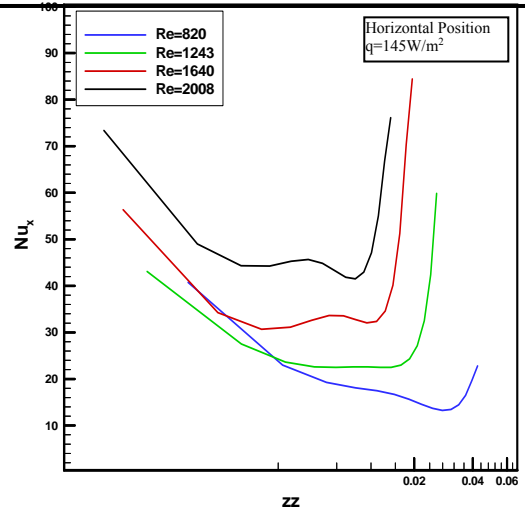


Fig.(15): Experimental Local Nusselt number Versus Dimensionless Axial Distance, $q=145\text{W/m}^2$, $\alpha = 0^\circ$ (Horizontal).

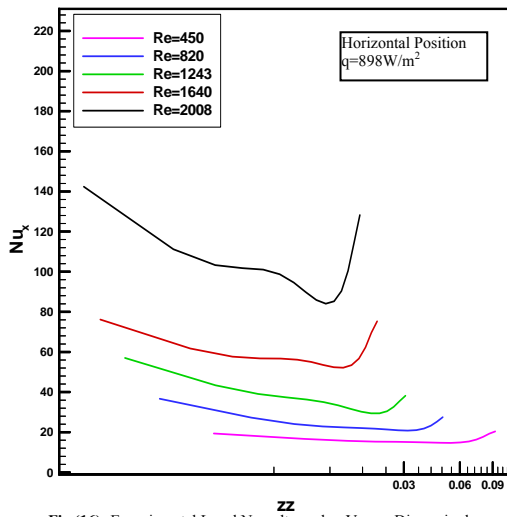


Fig.(16): Experimental Local Nusselt number Versus Dimensionless Axial Distance, $q=898\text{W/m}^2$, $\alpha = 0^\circ$ (Horizontal).

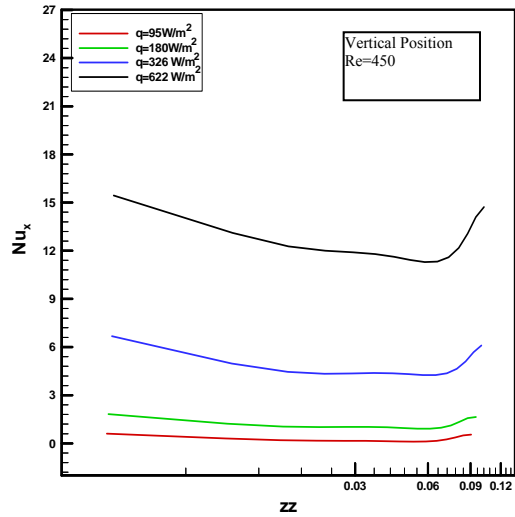


Fig.(17): Experimental Local Nusselt number Versus Dimensionless Axial Distance, $Re=450$, $\alpha = 90^\circ$ (Vertical).

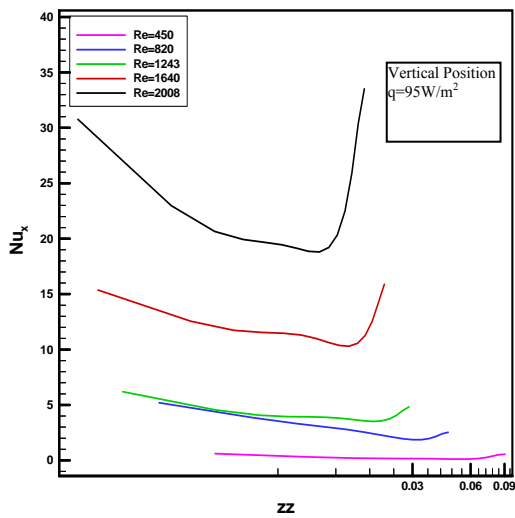


Fig.(18): Experimental Local Nusselt number Versus Dimensionless Axial Distance, $q=95\text{W/m}^2$, $\alpha = 90^\circ$ (Vertical).

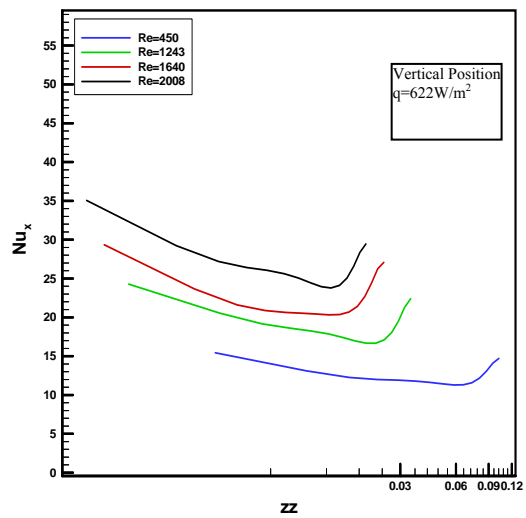


Fig.(19): Experimental Local Nusselt number Versus Dimensionless Axial Distance, $q=622\text{W/m}^2$, $\alpha = 90^\circ$ (Vertical).

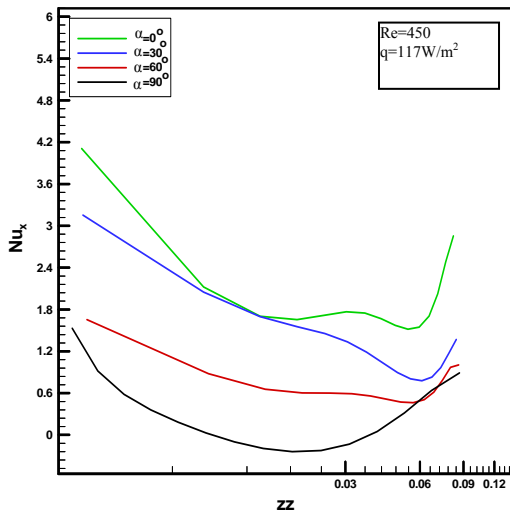


Fig.(20): Experimental Local Nusselt number Versus Dimensionless Axial Distance for Various Angles, Re=450, q=117W/m²

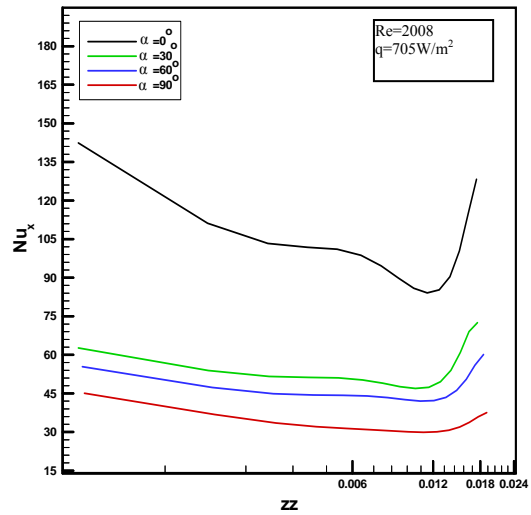


Fig.(21): Experimental Local Nusselt number Versus Dimensionless Axial Distance for Various Angles, Re=2008, q=705W/m²

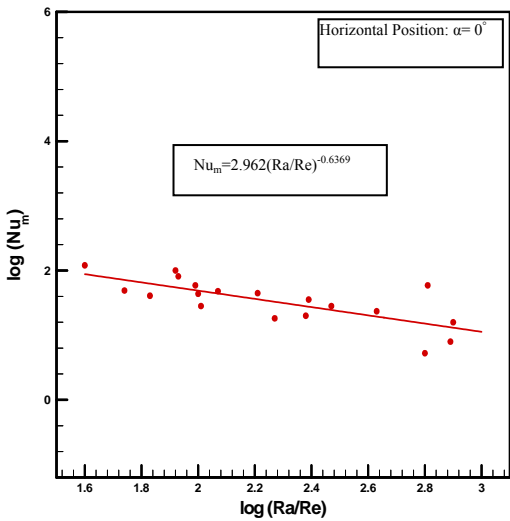


Fig.(22): Experimental Average Nusselt number Versus Ra/Re For $\alpha = 0^\circ$ (Horizontal Position).

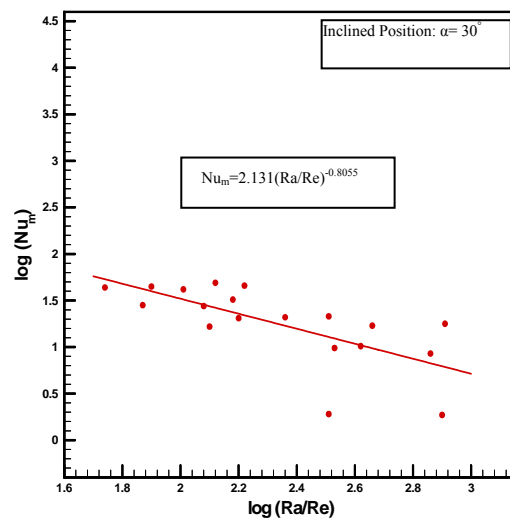


Fig.(23): Experimental Average Nusselt number Versus Ra/Re For $\alpha = 30^\circ$ (Inclined Position).

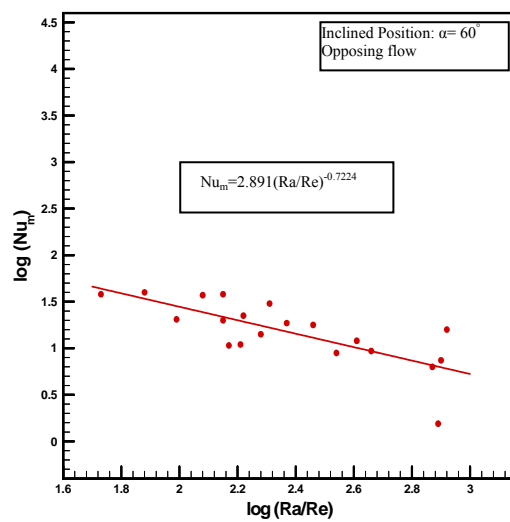


Fig.(24): Experimental Average Nusselt number Versus Ra/Re For $\alpha = 60^\circ$ (Inclined Position)

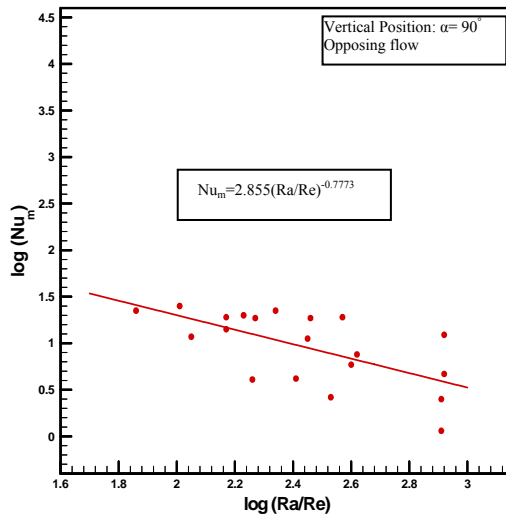


Fig.(25): Experimental Average Nusselt number Versus Ra/Re For $\alpha = 90^\circ$ (Vertical Position)